International Journal of Mechanical and Industrial Technology ISSN 2348-7593 (Online)
Vol. 3, Issue 1, pp: (338-343), Month: April 2015 - September 2015, Available at: www.researchpublish.com

Assessment on the Critical Failure Load of a Composite Structure with a Hole Reinforced Using Secondary Bonding

Hari Krishnan G.[1], Dr. Ramesh Kumar R[2], Dr. K. C. Gopalakrishnan[3]

[1]M. Tech Scholar, [2]Professor Government Engineering College Barton Hill, [3]Associate Professor, College Of Engineering Trivandrum, Kerala, India - 695035

Abstract: **Analysis of honeycomb sandwich payload adapter under equivalent axial compression load with secondary bonding for the reinforced hole is carried out based on CZM approach using tested fracture properties. For the structurally qualified design ultimate load, both post test NDT and CZM results, did not show the occurrence of any debonds. The parametric study shows that when the normal debond strength of the adhesive between the primary shell skin to secondary reinforcement around the hole reduces from the design configuration value of 20 MPa to a very low value of 3MPa, incipient of debond occurs on the tensile region of the hole retaining almost the critical buckling capability. With 2MPa normal bond strength, the failure load reduces by 12.7% and with 1MPa; the failure load reduces by 37%. Present study establishes in bringing out the minimum bond strength required for a secondary bond around holes following an equivalent solid honeycomb core model.**

Keywords: **CZM model, FWT value – Interfacial normal bond strength, honeycomb core.**

I. INTRODUCTION

CFRP skinned sandwich structures in the form of cylinder or cone with very thin skin thickness of 0.5mm and different diameters in the range of 1000 to 5000 mm with stubby to slender configurations that are designed to bear compressive loads are widely used in launch vehicles. Many investigators considered cohesive zone model analyses for the progressive failure adhesive joints [1-5]. Interfacial debond growth between honeycomb core and skin is generally very complex in nature, not only due to geometric and material nonlinearity but also the oscillatory singularity nature of stress and displacement field in the vicinity of the debond tip. . It was reported in literature that debond growth does not occur until the debond region has buckled and the growth is governed by the peel mode of fracture [4]. Honeycomb core is considered as equivalent material and good agreement was obtained with 3-D analysis as reported in Ref 6. Buckling analysis of stringer stiffened composite panel using well-known MCCI approach was studied and the critical load at which separation of the panel from stringer was evaluated [7]. Recent studies on the prediction of the initiation and progressive failure of composite and metallic sandwich beams using CZM analysis with experimental verification showed that the among fracture properties of adhesive, mode I and mode II delamination fracture toughness have less effect on failure mode when compared to interfacial normal strength (FWT value) [8 - 9]. Further, reinforcement around the hole bonded with room temperature curable adhesive having low lap shear strength (as a part of repair scheme) is considered for the study to assess the buckling induced peel stress at the debond front. The study is useful in the design of composite structure where need for a secondary bond for reinforcement is a mandatory.

In the present study, metallic skinned and composite skinned honeycomb sandwich adapters with different values of interfacial normal bond strength for a secondary bonding around holes are analyzed using cohesive zone model to arrive at a minimum required FWT value corresponding to the incipient of a debond so as to meet the design ultimate load considering the tested fracture properties of the adhesive.

II. COHESIVE ZONE MODEL – GENERAL THEORY

The cohesive zone model (CZM) approach has been widely accepted as an alternative to linear elastic fracture mechanics (LEFM) and is a computationally convenient fracture and failure analysis tool. The CZM approach within finite element analysis can predict the crack initiation, growth and direction of growth automatically. It is a highly nonlinear damage mechanics model able to describe the material behavior in the process zone ahead of a crack or delamination, leading to material separation at the crack tip. One of the important advantages of cohesive model is connected with their capacity to simulate onset and non-self-similar growth of damage without any pre-existing crack or debond. The method is based on a softening relationship between stresses and relative displacements between delaminated surfaces, thus simulating a gradual degradation of material properties. In finite element method cohesive elements compactable with the solid finite elements are used for the implementation of cohesive zone models as shown in Figure 1. In 2-D two line segments separated by a thickness is used as the cohesive interface elements. In 3-D which consists of two surfaces separated by a thickness, the relative motion of the top and bottom parts with respect to the element mid plane is treated as transverse shear behavior of the cohesive element. The relative motion of these parts of the cohesive element in the thickness direction represents the opening and closing of the interface element. The shearing and stretching of the element mid plane are associated with membrane strain.

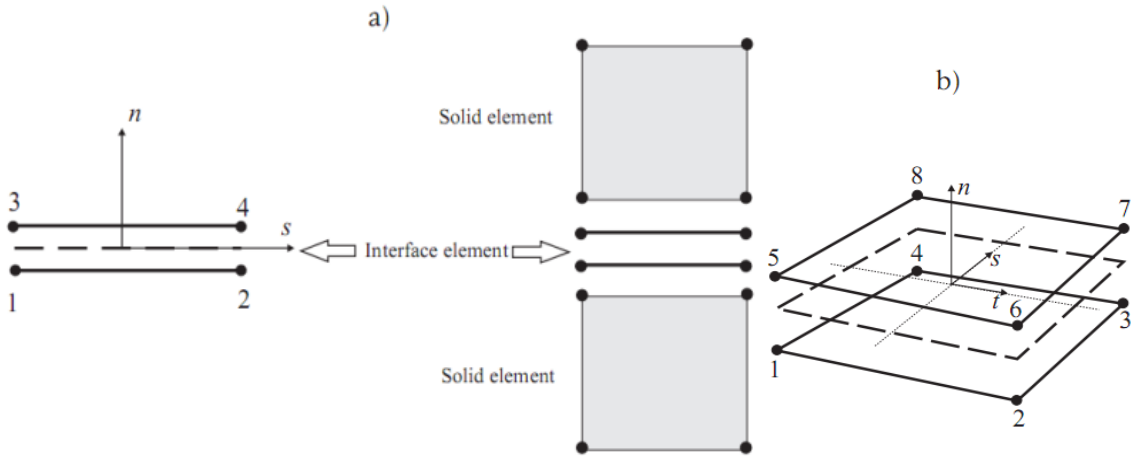

Figure 1: Schematic of cohesive elements: a) 2-D 4-node b) 3D 8-node

The cohesive element response depends on the specific application and the delamination is modeled based on the traction separation description of the interface. Traction separation model assumes linear elastic behavior in ABAQUS. The elastic constitutive tensor K_0 relates the traction vector σ to the opening displacement vector δ across the interface. For conventional materials damage of traction separation response is defined in Continuum Damage Mechanics. The damage mechanisms of the material consist of a damage initiation criterion, a damage evolution law and a propagation condition. Figure 2, shows a simple bilinear traction separation law written in terms of the effective traction σ and effective displacement δ.

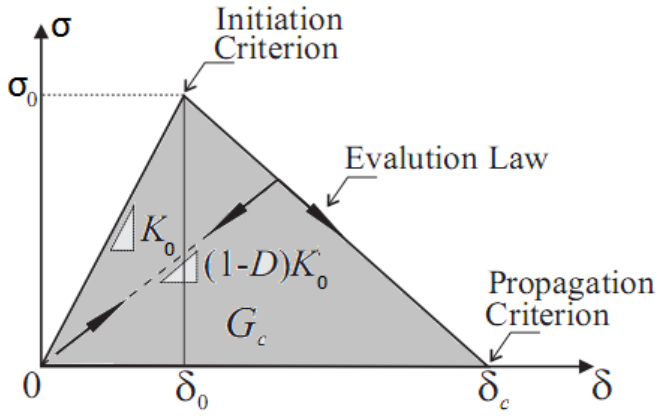

Figure 2: Traction-Separation behavior

The effective traction relates the effective displacement by three parameters, the peak traction σ_0 (local strength of the material), the displacement at the onset of damage δ_0, energy needed for opening the crack G_c (area under traction separation curve). Several damage initiation criteria are available in ABAQUS code. Once the damage initiation criterion is reached, the degradation of the material stiffness is specified by damage evolution law. The overall material damage is specified by a scalar damage variable D ($0 \leq D \leq 1$), which describe the damage evolution by under a combination of normal and shear deformation across the interface. When the damage variable reaches its maximum value (D = 1) corresponds to complete fracture of the interface layers which represents the delamination propagation. [9-10].

Needleman [1] proposed the model by assuming a scalar decohesion potential Φ in the form:

$$\phi(\Delta) = \phi_n + \phi_n \exp(-\frac{\Delta_n}{\delta_n})\left\{\left[1 - r + \frac{\Delta_n}{\delta_n}\right]\frac{(1-q)}{(r-1)} - \left[q + \frac{(r-q)\Delta_n}{(r-1)\delta_n}\right]\exp\left(-\Delta_t^2\right)\right\}$$

From which the cohesive traction force can be obtained as

$$T = -\frac{\partial \phi}{\partial \Delta}$$

where $T = [T_n, T_t]$ is traction vector and $\Delta = [\Delta_n, \Delta_t]$ is the displacement vector across the cohesive surface in normal and tangential directions. The parameters φn and φ_t are the energies required and Δ_n and Δ_t are the critical separations in pure normal and tangential, directions respectively. The parameters for normal and tangential separation, respectively, which are related to the cohesive normal strength σ_{max} and the tangential strength τ_{max} as

$$\phi_n = e\sigma_{\max}\delta_n$$

$$\phi_t = \sqrt{\frac{e}{2\tau_{\max}}}\delta_t$$

$$q = \frac{\phi_t}{\phi_n}$$

q - is the energy ratio and r is defined as the value of Δ_n/δ_n after complete shear separation with $T_n = 0$.

III. NUMERICAL RESULTS AND DISCUSSION

To begin with, buckling analysis of metallic sandwich adapter without any hole is analyzed using plate shell element and 3-D brick element, (without any interface elements) to establish the accuracy on critical buckling load for the full model and quarter model. The critical buckling load obtained for the full shell model based on 2-D analysis is 561kN while from the 3-D analysis is 607kN (Table-1). Deviation of 8% in the critical buckling loads observed between the two approaches is mainly due to honeycomb core properties taken for the analyses. It may be noted that for the 2-D analysis using plate – shell element with six degrees of freedom per node, the critical buckling load is obtained based on considering the tested properties for the transverse shear modulii while for the 3-D brick element equivalent properties of honeycomb core is based on density ratios of core and aluminium material. Moreover simulation of end rings to shell joints is appropriate in the latter case. The deviation in the buckling load for full 360 degree models and quarter, 90 degree models are very small with identical global buckling mode (Fig. 2).

Based on the CZM model as described in the method of approach in Sec. 2., it is observed from the present study that the critical failure load for the thermally cured resin system with FWT value of 20MPa for both primary (skin to core) and secondary reinforcement to skin is 564kN without any adhesive failure causing a debond in any of the interfaces. It may be noted that metallic sandwich adapter was earlier tested for 350kN equivalent axial compressive load that did not show any post test debond observations. The failure loads and mode of failures for various values for the secondary bond strength is given in Table-2. In case of composite adapter, failure load becomes 424kN corresponding to the case with maximum adhesive strength and fracture properties. It may be concluded that the circumferential stiffness plays an important role on the critical buckling strength which is less in the case of composite adapter when compared to metallic adapter.

TABLE I: EVALUATION OF CRITICAL BUCKLING LOAD BASED ON 2-D AND 3-D ANALYSIS

	Critical buckling load in kN	
	Full model (360^0)	**Quarter model (90^0)**
2-D analysis using plate/shell element	561kN	560 kN
3-D analysis using brick element	607 kN	595kN

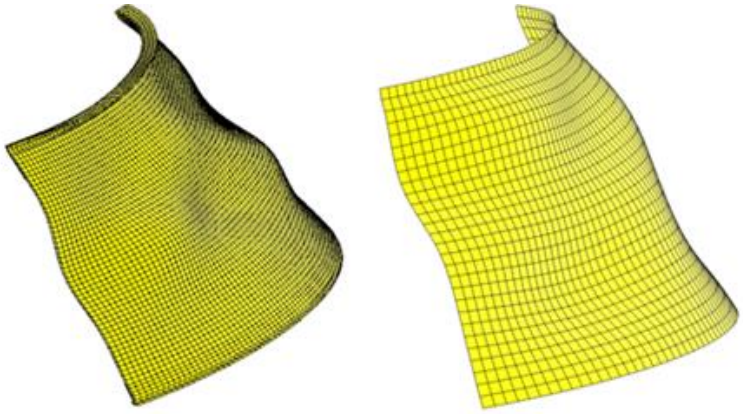

(a) **(b)**

Figure 2. Buckling modes of (a) 2-D and (b) 3-D models of sandwich adapter

Fig. 3 shows stresses corresponding to the failure load in metallic adapter. Honeycomb core shear stress estimated back is 0.72MPa as against 0.75MPa based on the equivalent core properties taken.

When the interfacial normal strength, between the reinforcement and inner skin, becomes 3MPa debond initiation occurs (Table-2.). The failure load marginally reduces by 15%. In the case of CFRP skinned sandwich adapter, similar reduction occurs much higher FWT value of 5MPa with much drop in the failure load. However, as expected both the adapters show a similar failure load once the FWT values reduces significantly.

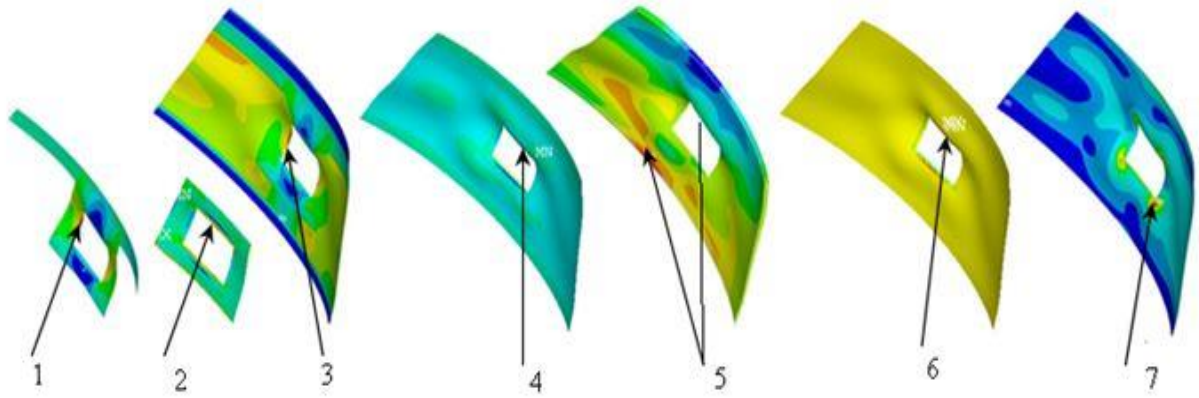

1. Maximum stress in the reinforcement skin - 320MPa
2. Maximum stress in the adhesive - 3MPa
3. Maximum stress in the inner skin - 334MPa
4. Maximum stress in the adhesive - 2.80MPa
5. Maximum stress in the core - 0.72MPa
6. Maximum stress in the adhesive - 2.68MPa
7. Maximum stress in the outer skin - 283MPa

Figure 3 Stresses in the metallic skinned sandwich adapter.

TABLE II CRITICAL FAILURE LOAD AND MODE OF FAILURE IN METALLIC AND COMPOSITE SANDWICH ADAPTERS FOR DIFFERENT INTERFACE SECONDARY BOND PROPERTIES

Skin-Core Interface strength. FWT-6MPa	Reinforcement skin to shell skin Interface Strength (Lap shear strength, MPa)	Peak Load kN	Mode of failure	Interface Opening of Adhesive layer (mm)	
				Inner Skin to core	Reinforcement to inner skin
Metallic sandwich adapter	20	564	Global buckling	Nil	Nil
	10	564			
	6	564			
	5	564			
	4	564			
	3	480	Adhesive Failure		0.058
	2	430		0.062	0.185
	1	208		0.084	0.256
Composite sandwich adapter	20	424	Global buckling	Nil	Nil
	10	424			Nil
	6	424			Nil
	5	418			0.052
	4	403			0.057
	3	388	Adhesive Failure	0.052	0.058
	2	357		0.076	0.122
	1	201		0.084	0.187

It may be noted from Fig. 4, that separation or debond of adhesive has taken place in the tensile region of the cutout as expected. The critical load for the metallic adapter is 480kN as against 418kN for the composite adapter.

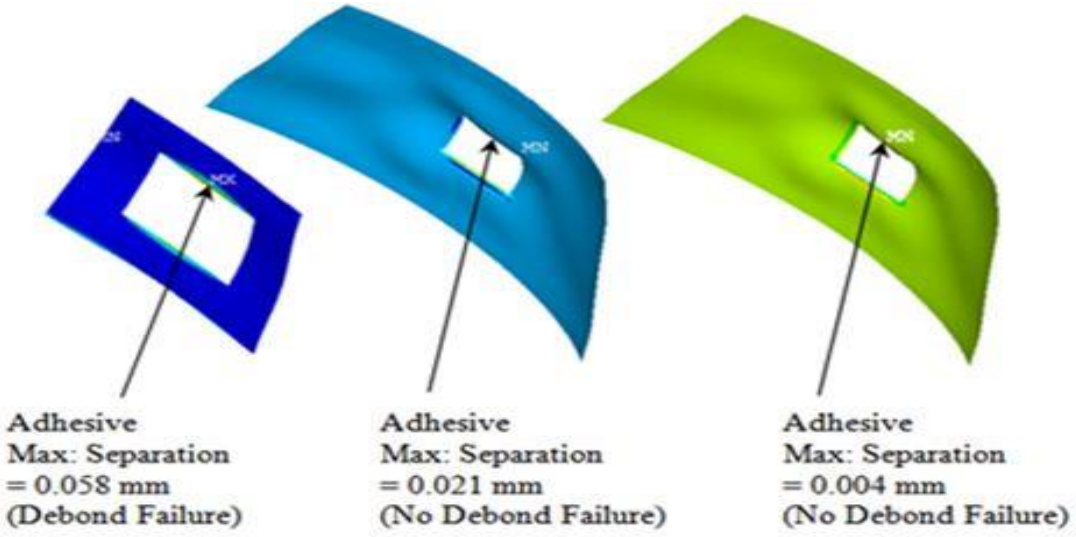

Fig. 4. Adhesive separation at three interfaces in the metallic skinned sandwich adapter.

IV. CONCLUSIONS

Coupled buckling induced delamination of secondary bonding of the reinforcement around hole in aluminium skinned honeycomb sandwich adapter as well as carbon epoxy skinned sandwich adapter have been simulated using cohesive zone model. Structural integrity of metallic sandwich adapter which was assessed earlier based on post test NDT has been established using CZM approach followed in the present study. Out of the three major fracture properties of adhesive, FWT value for the secondary bonding is varied from 20MPa to 1 MPa retaining the approved tested value for interface between core and skin and critical buckling load at which adhesive failure occurs in the secondary debond have been

captured. For a given axial stiffness and mass, minimum adhesive strength to avoid secondary debond failure should be above 3MPa in the case of metallic sandwich adapter while it is 5MPa for the composite adapter. It is concluded that such difference is due to the less circumferential stiffness of composite adapter when compared to metallic adapter. It may also be concluded that as long as secondary bond interfacial normal strength is higher than adhesive strength at which separation occurs, metallic adapter will have higher failure load than that of composite adapter configuration considered.

REFERENCES

[1] Needleman, A., A continuum model for void nucleation by inclusion debonding, Journal of Applied Mechanics, 54 (1987), pp. 25-531.

[2] Alfano, Furgiuele, Leonardi, Maletta, Paulino Fracture analysis of adhesive Jointsusing intrinsic cohesive zone models, Key Eng Mat, 348, (2007), pp.13-16.

[3] B. R. Blackman., H.Hadavinia, The use of cohesive zone model to study the fracture of fiber composites and adhesively bonded joints, International Journal of Fracture, (2003) 119:25-46.

[4] L. A. Carlsson, L. S. Sendlein and Merry, Characterization of face sheet/core shear fracture of composites sandwichbeams,Journal of Composite materials, (1991) 25:101- 116.

[5] M. Burman, Fatigue crack initiation and propagation in sandwich structures. PhD thesis, Royal Institute of Technology, Sweden. (1998).

[6] R. Aitken-Damage due to soft body impact on composite sandwich aircraft Panels, PhD thesis, The University of Auckland, New Zealand (2000).

[7] R.Rameshkumar, K. S. Praveen and Venkateswara Rao Assessment of Delamination Fracture Load of Stringer Stiffened Composite Panel, AIAA Journal, 3(2003), pp. 551- 553.

[8] K. C. Gopalakrishnan and R Rameshkumar, Failure assessment of CFRP skinned honeycomb sandwich beam with delamination using cohesive zone model, International Journal of Engineering Research and Applications, 3(2011) , pp. 1040-1050.

[9] K. C. Gopalakrishnan, R. Rameshkumar and S. Anil Lal Cohesive zone modeling of coupled buckling - Debond growth in metallic honeycomb sandwich structure, Journal of Sandwich Structures and Materials, 14(2012), pp. 679-693.

[10] Alfano G, Crisfield MA. Solution strategies for the delaminationanalysis based on a combination of local-control arc length andline searches. Int J Numer Meth Eng 2003;58(7):999–1048

[11] Alfano G, Crisfield MA. Delamination analysis via interface elements: mixed-mode and local control solution algorithms. I.C. Aero Report 99-05, Imperial College, London, 1999